Decoy-state quantum key distribution with two-way classical postprocessing

Xiongfeng Ma,[1,*] Chi-Hang Fred Fung,[1,†] Frédéric Dupuis,[2,‡] Kai Chen,[1] Kiyoshi Tamaki,[3,§] and Hoi-Kwong Lo[1,‖]

[1]*Center for Quantum Information and Quantum Control, Department of Physics and Department of Electrical & Computer Engineering, University of Toronto, Toronto, Ontario, Canada M5S 1A7*

[2]*Département IRO, Université de Montréal, Montréal, Québec, Canada H3C 3J7*

[3]*NTT Basic Research Laboratories, NTT Corporation, 3-1, Morinosato Wakamiya Atsugi-Shi, Kanagawa, 243-0198, and CREST, JST Agency, 4-1-8 Honcho, Kawaguchi, Saitama, 332-0012, Japan*

Decoy states have recently been proposed as a useful method for substantially improving the performance of quantum key distribution (QKD) protocols when a coherent-state source is used. Previously, data postprocessing schemes based on one-way classical communications were considered for use with decoy states. In this paper, we develop two data postprocessing schemes for the decoy-state method using two-way classical communications. Our numerical simulation (using parameters from a specific QKD experiment as an example) results show that our scheme is able to extend the maximal secure distance from 142 km (using only one-way classical communications with decoy states) to 181 km. The second scheme is able to achieve a 10% greater key generation rate in the whole regime of distances. We conclude that decoy-state QKD with two-way classical postprocessing is of practical interest.

PACS number(s): 03.67.Dd, 03.67.−a, 03.67.Hk

I. INTRODUCTION

Quantum key distribution (QKD) allows two users, commonly called Alice (sender) and Bob (receiver), to communicate in absolute security in the presence of an eavesdropper Eve. Unlike classical cryptography, the security of QKD is based on the fundamental principles of quantum mechanics, rather than unproven computational assumptions.

The best-known QKD protocol—the Bennett-Brassard 1984 (BB84) scheme—was published in 1984 [1]. In the BB84 protocol, Alice sends Bob a sequence of single photons each of which is randomly prepared in one of two conjugate bases. Bob measures each photon randomly in one of two conjugate bases. Alice and Bob then publicly compare the bases and keep only those results (bits) for which they have used the same basis. They randomly test a subset of those bits and determine the quantum bit error rate (QBER). If the QBER is larger than some prescribed value, they abort the protocol. Otherwise, they proceed to the classical data postprocessing (which consists of error correction and privacy amplification) and generate a secure key. The security of the BB84 protocol has been rigorously proven in a number of papers [2–4]; see also [5].

The security proof in [4] shows that the BB84 protocol can be successively reduced from an entanglement distillation protocol (EDP). This idea is relevant to this paper since our data postprocessing schemes are based on EDPs. We remark that the EDP was first discussed in [6], that its relevance to the security of QKD was emphasized in [7], and that this connection was established rigorously in [3]. The EDPs proposed earlier use local operations and one-way classical communication (1-LOCC). Later, Gottesman and Lo provided security proofs of standard quantum key distribution schemes by using an EDP with local operations and two-way classical communication (2-LOCC) [8]. They showed that the BB84 protocol using 2-LOCC can tolerate a higher bit error rate than 1-LOCC (see also [9]). On the other hand, Gerd, Vollbrecht, and Verstraete proposed another EDP that uses a 2-LOCC-based recurrence scheme [10]. Although their scheme was originally proposed as an EDP, we will use it here in a QKD to increase the key generation rate. (It should be noted that the EDP approach is only one of several approaches to security proofs of QKD. Other useful approaches to security proof can be based on, for example, communication complexity [11], quantum memory [12,13], or direct information-theoretic argument [14].) Recently, it has been demonstrated [15] rigorously that one can generate a long secure key even when the amount of distillable entanglement in a quantum state is arbitrarily small. In other words, secure key generation is strictly weaker than entanglement distillation. The universal composability of quantum key distribution has been proven in [16].

In summary, QKD is secure in theory. Much of the interest in QKD is due to its potential in near-term real-life applications. Indeed, commercial optical-fiber-based quantum cryptographic products are already on the market [17].

Meanwhile, experimentalists have done many QKD experiments, such as [18–20]. The key issue in QKD experiments is whether they are really secure. Standard security proofs are often based on perfect devices, such as perfect single-photon sources. All devices are imperfect in real implementations, such as imperfect single-photon sources and highly lossy channels. It is thus important to study the security of QKD with imperfect devices. Substantial progress has been made in the subject [21–24].

Unfortunately, with the method of Gottesman, Lo, Lütkenhaus, and Preskill (GLLP) [23], QKD can only be proven to be secure at very limited key generation rates and dis-

*Electronic address: xima@physics.utoronto.ca

†Electronic address: cffung@comm.utoronto.ca

‡Electronic address: dupuisf@iro.umontreal.ca

§Electronic address: tamaki@will.brl.ntt.co.jp

‖Electronic address: hklo@comm.utoronto.ca

tances. It came as a big surprise that a simple solution to the problem—the decoy-state method—actually exists. The decoy method was first discovered by Hwang [25], and made rigorous by Lo and co-workers [26,27], and also [28,29]. In addition, Zhao *et al.* demonstrated experimental implementation of a QKD protocol using one decoy state [30].

The usefulness of decoy-state protocols over non-decoy-state protocols has previously been demonstrated [26,27], within the context of 1-LOCC, for an imperfect source. Since 2-LOCC is known to be superior to 1-LOCC for a perfect source [8–10], it would be interesting to study the usefulness of decoy-state protocols with 2-LOCC, for an imperfect source. This is the main goal of this paper. Indeed, as we will show, decoy-state protocols with 2-LOCC are superior to decoy-state protocols with only 1-LOCC in realistic situations. Specifically, in this paper, we develop two data post-processing schemes for the decoy method of [26,27] by applying two 2-LOCC EDPs, the Gottesman-Lo EDP [8] and the recurrence scheme [10]. Both methods are superior to the random hashing 1-LOCC EDP (for the rest of the paper, we will simply call this the 1-LOCC EDP) with ideal devices in two different aspects: the Gottesman-Lo EDP was shown to be able to achieve a higher tolerable bit error rate, while the recurrence method was shown to be able to achieve a higher key generation rate. We will show in this paper that the same conclusion holds in the case of imperfect devices. In particular, depending on the distance in a QKD experiment, one can use our Gottesman-Lo EDP-based data post-processing scheme in the long-distance region or our recurrence-based data postprocessing scheme in the short-distance region to increase the key generation rate.

We note that a recent and independent analysis of combining B steps with the GLLP method and decoy states is given in [31]. That data postprocessing scheme is the same as our first scheme, which is aimed at increasing the maximal secure distance. On the other hand, in this paper, we also propose a second scheme, which is aimed at increasing the key rate at short distances.

The organization of this paper is as follows. We first review entanglement distillation in Sec. II and some existing techniques for realistic QKD in Sec. III. We then investigate the tolerable error rates and the upper bounds of secure distance and key generation rate in Sec. IV. Sections V and VI contain the main results of the paper. Specifically, we develop two data postprocessing schemes, one with the B steps from Gottesman and Lo [8] (see Sec. V), and the other with recurrence (see Sec. VI). Our simulation (based on the Gobby-Yuan-Shields (GYS) experiment [19]) shows that with B steps from the Gottesman-Lo EDP, the maximal secure distance can be extended to 180 km compared with 140 km with 1-LOCC, and the key generation rate increased by more than 10% in the whole regime of distances. With our QKD model, we also consider statistical fluctuations on the estimated parameters when the data have finite length (see Sec. VII). The result shows that the B step can extend the maximal secure distance and the recurrence can raise the key generation rate after taking statistical fluctuations into account. Although, in this paper, we focus on the BB84 protocol, our schemes can be applied to other QKD protocols as well.

II. REVIEW OF ENTANGLEMENT DISTILLATION

In this section, we review Shor and Preskill's security proof of QKD and two EDPs based on 2-LOCC (the Gottesman-Lo and recurrence EDPs) assuming that ideal single-photon sources are used. In Secs. V and VI, we generalize these two schemes for realistic setups.

The idea of the Shor-Preskill [4] security proof of QKD is to apply an EDP to show that the leaked information about the final key is negligible. Here we will explain how to analyze the security of EDP-based QKD.

In the EDP-based QKD protocol, Alice creates $n+m$ pairs of qubits, each in the state

$$|\psi\rangle = \frac{1}{\sqrt{2}}(|00\rangle + |11\rangle),$$

the eigenstate with eigenvalue 1 of the two commuting operators $X \otimes X$ and $Z \otimes Z$, where

$$X = \begin{pmatrix} 0 & 1 \\ 1 & 0 \end{pmatrix}, \quad Z = \begin{pmatrix} 1 & 0 \\ 0 & -1 \end{pmatrix}$$

are the Pauli operators. Then she sends half of each pair to Bob. Alice and Bob sacrifice m randomly selected pairs to test the error rates in the X and Z bases by measuring $X \otimes X$ and $Z \otimes Z$. If the error rates are too high, they abort the protocol. Otherwise, they conduct the EDP, extracting k high-fidelity pairs from the n noisy pairs. Finally, Alice and Bob both measure Z on each of these pairs, producing a k-bit shared random key about which Eve has negligible information. The protocol is secure because the EDP removes Eve's entanglement with the pairs, leaving her negligible knowledge about the outcome of the measurements by Alice and Bob.

In the EDP, after the qubits' transmission, Alice and Bob will share the state with density matrix

$$\rho = \begin{pmatrix} q_{00} & \times & \times & \times \\ \times & q_{10} & \times & \times \\ \times & \times & q_{11} & \times \\ \times & \times & \times & q_{01} \end{pmatrix}, \quad (1)$$

normalized with $q_{00}+q_{10}+q_{11}+q_{01}=1$. Here the x's denote arbitrary numbers, all of which are not necessarily the same, and the density matrix is in the Bell basis:

$$|\psi_{00}\rangle = \frac{1}{\sqrt{2}}(|00\rangle + |11\rangle),$$

$$|\psi_{10}\rangle = \frac{1}{\sqrt{2}}(|01\rangle + |10\rangle),$$

$$|\psi_{11}\rangle = \frac{1}{\sqrt{2}}(|01\rangle - |10\rangle),$$

$$|\psi_{01}\rangle = \frac{1}{\sqrt{2}}(|00\rangle - |11\rangle). \tag{2}$$

Since the EDPs we consider in this paper do not make use of the off-diagonal elements in Eq. (1) to extract entanglement, it is sufficient to characterize the density matrix by only the diagonal elements $(q_{00}, q_{10}, q_{11}, q_{01})$. In fact, any shared state can always be transformed into a diagonal form by local operations and classical communications [32]. The density matrix is now a classical mixture of the Bell states ψ_{ij} with probabilities q_{ij}. Therefore, the bit and phase error rates are given by

$$\delta_b = q_{10} + q_{11},$$

$$\delta_p = q_{11} + q_{01}. \tag{3}$$

A QKD protocol based on a Calderbank-Shor-Steane (CSS) [33] EDPs can be reduced to a "prepare-and-measure" protocol (BB84) [4]. CSS codes correct bit errors and phase errors separately, which respectively turn out to be the bit error correction and privacy amplification in the context of QKD [4]. Thus the key rate of this 1-LOCC based data post-processing scheme is given by [4,34],

$$R_{CSS} = q[1 - H_2(\delta_b) - H_2(\delta_p)], \tag{4}$$

where q depends on the implementation (1/2 for the BB84 protocol, because half the time Alice and Bob bases are not compatible, and if we use the efficient BB84 protocol [35], we can have $q \approx 1$), δ_b and δ_p are the bit flip error rate and the phase flip error rate, and $H_2(x)$ is the binary entropy function,

$$H_2(x) = -x\log_2(x) - (1-x)\log_2(1-x).$$

In summary, there are two main parts of the EDPs: bit flip error correction (for error correction) and phase flip error correction (for privacy amplification). These two steps can be understood as follows. First Alice and Bob apply an error correction, after which they share the same key strings but Eve may still keep some information about the key. Alice and Bob then perform the privacy amplification to expunge Eve's information from the key. We remark that the key generation rate achieved by Eq. (4) requires only 1-LOCC.

A. Gottesman-Lo EDP

Gottesman and Lo [8] introduced an EDP based on 2-LOCC for use with QKD and showed that it can tolerate a higher bit error rate than 1-LOCC based EDP's. B and P steps are two primitives in the Gottesman-Lo EDP, and the EDP consists of executing a sequence of B and/or P steps, followed by random hashing. The random hashing part is a 1-LOCC EDP. The main objective for the extra B and P steps is to reduce the bit and/or phase error rates of qubits so that the random hashing can work to extract secure keys. This is the reason why the Gottesman-Lo EDP is able to tolerate a higher initial bit error rate than 1-LOCC EDPs. The definitions of B and P steps are as follows.

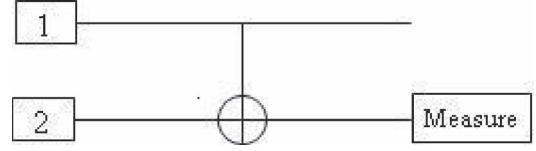*Definition of B step [8].* This is shown in Fig. 1. After

FIG. 1. Alice and Bob choose two half EPR pairs and input the quantum circuit as shown above. They discard both control and target qubits if they disagree on the outcomes of measurement on the target qubits. On the other hand, they keep the control qubits as surviving qubits if their measurement outcomes agree.

randomly permuting all the Einstein-Podolsky-Rosen (EPR) pairs, Alice and Bob perform a bilateral XOR (BXOR) operation between EPR pairs and measure the target qubits in the Z basis. This effectively measures the operator $Z \otimes Z$ for each of Alice and Bob, and detects the presence of a single bit-flip error. If Alice's and Bob's measurement outcomes disagree, they discard the remaining EPR pair; otherwise, they keep the control qubit.

Since the B step involves only the measurement of $Z \otimes Z$, it can be used in the prepare-and-measure BB84 protocol. Classically, the B step simply involves random pairing of the key bits, say x_1, x_2 on Alice's side and y_1, y_2 on Bob's side, and the computation of the parity of each pair of bits, $x_1 \oplus x_2$ and $y_1 \oplus y_2$. Both Alice and Bob announce the parities. If their parities are the same, they keep x_1 and y_1; otherwise, they discard x_1, x_2, y_1, and y_2. We can see that the B step is very simple to implement in data postprocessing.

Suppose Alice and Bob input a control qubit $(q_{00}^C, q_{10}^C, q_{11}^C, q_{01}^C)$ and a target qubit $(q_{00}^T, q_{10}^T, q_{11}^T, q_{01}^T)$ with bit error rates δ_b^C and δ_b^T and phase error rates δ_p^C and δ_p^T, respectively. After one B step, the survival probability p_S is given by

$$p_S = (q_{00}^C + q_{01}^C)(q_{00}^T + q_{01}^T) + (q_{10}^C + q_{11}^C)(q_{10}^T + q_{11}^T)$$
$$= (1 - \delta_b^C)(1 - \delta_b^T) + \delta_b^C \delta_b^T, \tag{5}$$

and the density matrix $(q_{00}', q_{10}', q_{11}', q_{01}')$ of the output control qubit is given by

$$q_{00}' = \frac{q_{00}^C q_{00}^T + q_{01}^C q_{01}^T}{p_S},$$

$$q_{10}' = \frac{q_{10}^C q_{10}^T + q_{11}^C q_{11}^T}{p_S},$$

$$q_{11}' = \frac{q_{10}^C q_{11}^T + q_{11}^C q_{10}^T}{p_S},$$

$$q_{01}' = \frac{q_{00}^C q_{01}^T + q_{01}^C q_{00}^T}{p_S}. \tag{6}$$

Equations (6) can be derived from Table II of [32]. The corresponding bit error rate δ_b and phase error rate δ_p can be obtained from Eq. (6) by

$$\delta_b' = q_{10}' + q_{11}' = \frac{\delta_b^C \delta_b^T}{p_S},$$

$$\delta_p' = q_{11}' + q_{01}'. \tag{7}$$

Definition of P step [8]. Randomly permute all the EPR pairs. Afterward, group the EPR pairs into sets of three, and measure $X_1 X_2$ and $X_1 X_3$ on each set (for both Alice and Bob). This can be done (for instance) by performing a Hadamard transform, two bilateral XOR operations, measurement of the last two EPR pairs, and a final Hadamard transform. If Alice and Bob disagree on one measurement, Bob concludes that the phase error was probably on one of the EPR pairs which was measured and does nothing; if both measurements disagree for Alice and Bob, Bob assumes that the phase error was on the surviving EPR pair and corrects it by performing a Z operation.

Without a quantum computer, Alice and Bob are not able to perform the P steps, so the EDP cannot depend on the results of P steps. When the P step is implemented classically in the BB84 protocol, the phase errors are not detected or corrected (i.e., the phase-flip operation Z is not applied). The P step then will be reduced as follows. Alice and Bob randomly form trios of the remaining qubits and compute the parity of each trio, say $x_1 \oplus x_2 \oplus x_3$ by Alice and $y_1 \oplus y_2 \oplus y_3$ by Bob. They now regard those parities as their new bits for further processing.

Since before P steps Alice and Bob will do random permutation, for simplicity, we assume the input three qubits have the same density matrix $(q_{00}, q_{10}, q_{11}, q_{01})$. After one P step, the density matrix $(q_{00}', q_{10}', q_{11}', q_{01}')$ of the output qubit is given by

$$q_{00}' = q_{00}^3 + 3q_{00}^2 q_{01} + 3q_{10}^2(q_{00} + q_{01}) + 6q_{00}q_{10}q_{11},$$

$$q_{10}' = q_{10}^3 + 3q_{10}^2 q_{11} + 3q_{00}^2(q_{10} + q_{11}) + 6q_{00}q_{10}q_{01},$$

$$q_{11}' = q_{11}^3 + 3q_{10}q_{11}^2 + 3q_{01}^2(q_{10} + q_{11}) + 6q_{00}q_{11}q_{01},$$

$$q_{01}' = q_{01}^3 + 3q_{00}q_{01}^2 + 3q_{11}^2(q_{00} + q_{01}) + 6q_{10}q_{11}q_{01}, \tag{8}$$

which is given in Appendix C of [8]. So the bit error rate and phase error rate will be given by

$$\delta_b' = q_{10}' + q_{11}' = 3\delta_b(1 - \delta_b)^2 + \delta_b^3,$$

$$\delta_p' = q_{11}' + q_{01}' = 3\delta_p^2(1 - \delta_p) + \delta_p^3. \tag{9}$$

Here we emphasize that the B and P steps are important elements of the Gottesman-Lo EDP. After B and P steps, the Gottesman-Lo EDP will be the same as the regular 1-LOCC EDP.

B. Recurrence EDP scheme

Here we review another two-way EDP, the recurrence scheme [10]. Similar to the B step in the Gottesman-Lo EDP, the recurrence scheme reduces the bit error rate of the EPR pairs before passing them to the 1-LOCC-based random hashing for the distillation of maximally entangled EPR pairs. However, there are two main differences between these two EDP schemes. The first is how the bit error syndrome of a target EPR pair in a bilateral XOR operation is learned. In the Gottesman-Lo EDP, Alice and Bob simply measure the target EPR pair in the Z basis and compare their results to learn the bit error syndrome (see Fig. 1). In the recurrence scheme, Alice and Bob group the bit error syndromes of all target EPR pairs together and learn all the syndromes using random hashing. The second difference is that the recurrence scheme requires some extra maximally entangled EPR pairs to begin with for learning the bit error syndromes, whereas no such extra pairs are required in the Gottesman-Lo EDP. We note that the recurrence methods have been studied in various papers, such as [7,36–38].

The steps for the recurrence protocol are as follows.

(1) Alice and Bob perform two BXOR operations on two noisy EPR pairs and one perfect maximally entangled EPR pair. Specifically, the first BXOR operation is performed on one noisy EPR pair as the source and the perfect EPR pair as the target, and the second BXOR operation is performed after the first BXOR operation using the other noisy EPR pair as the source and the same target.

(2) They do random hashing on the target EPR pairs to learn the parities of the noisy EPR pairs. Note that only a portion of the target EPR pairs have to be measured in order to learn all the parities. This is different from the B step approach.

(3) They do error correction and privacy amplification separately for even-parity and odd-parity EPR pairs.

In the prepare-and-measure scenario, the first two steps are as follows. Alice and Bob randomly pair up the key bits, and for each pair they compute the parity. They each compress their own sequence of parities by using random hashing, encrypt the resulting hash values using the one-time pad with some preshared secret bits, and send the encrypted results to each other. Note that they use the same sequence of secret bits to encrypt their own sequence of hash values. They learn the parities of the original noisy EPR pairs by adding the other party's encrypted sequence to their own encrypted sequence of hash values. Once they know the parities, they perform error correction and privacy amplification on the even-parity and odd-parity key bits separately. Note that the secret bits used up in the process should be returned to the secret bit pool by using the newly generated secret bits.

The key generation rate using the recurrence EDP with a single-photon source is given by

$$R = q\left[-\frac{1}{2}H_2(p_S) - \frac{1}{2}p_S H_2\left(\frac{\delta_b^C \delta_b^T}{p_S}\right) + K \right] \tag{10}$$

where q is defined similarly as in Eq. (4), p_S [given in Eq. (A2)] is the probability of getting even parity, and δ_b^C (δ_b^T) is the bit error rate of the control (target) EPR pair. Here, the first term in the brackets corresponds to the extra perfect EPR pairs borrowed, the second term corresponds to error correction, and the third term K [given in Eq. (A12)] corresponds to privacy amplification. In Appendix A, we review the recurrence EDP in detail and develop the key rate formula.

III. REVIEW OF REALISTIC QKD

In this section, we set up a model for realistic QKD, and review the ideas of the GLLP and decoy-state QKDs.

A. Realistic QKD setup

In this section, we present a widely used fiber-based QKD system model. All later simulations of QKD are based on this model. In order to describe a real-world QKD system, we need to model the source, transmission and detection following [21] (see also [27]).

1. Source

The laser source used in the QKD experiment can be modeled as a weak coherent state. Assuming that the phase of each pulse is totally randomized, the photon number of each pulse follows a Poisson distribution with a parameter μ as its expected photon number set by Alice. Thus, the density matrix of the state emitted by Alice is given by

$$\rho_A = \sum_{i=0}^{\infty} \frac{\mu^i}{i!} e^{-\mu} |i\rangle\langle i|, \tag{11}$$

where $|0\rangle\langle 0|$ is the vacuum state and $|i\rangle\langle i|$ is the density matrix of the i-photon state for $i=1,2,\ldots$. The states with only one photon ($i=1$) are normally called single-photon states. The states with more than one photon ($i\geq 2$), on the other hand, are called multiphoton states. Here, we assume Eve receives all the pulses sent by Alice. Eve performs some arbitrary operations and sends either a vacuum or a qubit to Bob. This is the squash operation introduced by GLLP [23]. Consequently, we denote the qubits coming from these three states as vacuum qubits, single-photon qubits, and multiphoton qubits.

A vacuum qubit is a qubit sent by Eve when Alice sent a vacuum state. (In the case without Eve's presence, it is some random qubit stemming from the dark counts of Bob's detector or other background contributions.) Thus, it does not contribute to the key generation. Due to photon-number splitting (PNS) attacks [39–42], multiphoton states are not secure for the BB84 protocol. Here is a key observation of this QKD model: the final secure key can be extracted only from single-photon qubits.[1] Besides the BB84 protocol, this is true for most present QKD protocols, such as the Ekert 1991 [44], the Bennett 1992 [45], and the six-state [46] protocols. One exception is the Scarani-Acin-Ribordy-Gisin 2004 (SARG04) protocol [47], in which two-photon states can also contribute to the secure key generation rate [43,48].

2. Transmission

For optical-fiber-based QKD systems, the losses in the quantum channel can be derived from the loss coefficient α

measured in dB/km and the length of the fiber l in km. The overall transmittance is given by

$$\eta = \eta_{Bob} 10^{-\alpha l/10}, \tag{12}$$

where η_{Bob} denotes the transmittance in Bob's side, including the internal transmittance of the optical components and detector efficiency. Here we assume a threshold single-photon detector on Bob's side. That is to say, we assume that Bob's detector can tell whether there is a click or not. However, it cannot tell the actual photon number of the received signal, if it contains at least one photon.

It is reasonable to assume independence between the behaviors of the i photons in i-photon states. Therefore the transmittance of an i-photon state η_i with respect to a threshold detector is given by

$$\eta_i = 1 - (1 - \eta)^i \tag{13}$$

for $i=0,1,2,\ldots$.

3. Yield

Define Y_i to be the yield of an i-photon state, i.e., the conditional probability of a detection event at Bob's side given that Alice sends out an i-photon state. Note that Y_0 is the background rate, which includes detector dark counts and other background contributions such as the stray light from timing pulses.

The yield of the i-photon state Y_i mainly comes from two parts, the background and the true signal. Assuming that the background counts are independent of the signal photon detection, then Y_i is given by

$$Y_i = Y_0 + \eta_i - Y_0 \eta_i \cong Y_0 + \eta_i. \tag{14}$$

Here we assume Y_0 (typically 10^{-5}) and η (typically 10^{-3}) are small.

The *gain* of an i-photon state Q_i is given by

$$Q_i = Y_i \frac{\mu^i}{i!} e^{-\mu}. \tag{15}$$

The gain Q_i is the product of the probability of Alice sending out an i-photon state (which follows a Poisson distribution) and the conditional probability of Alice's i-photon state (and background) that will lead to a detection event in Bob's detector.

4. Quantum bit error rate

The error rate of i-photon states e_i is given by

$$e_i = \frac{e_0 Y_0 + e_d \eta_i}{Y_i} \tag{16}$$

where e_d is the probability that a photon hits the erroneous detector. e_d characterizes the alignment and stability of the optical system. Experimentally, even at distances as long as 120 km, e_d is independent of the distance [19]. In what follows, we will also assume that e_d is independent of the transmission distance. We will assume that the background is random. Thus the error rate of the background is $e_0 = \frac{1}{2}$. Note that Eqs. (13)–(16) are satisfied for all $i=0,1,2,\ldots$.

---

[1] That only single-photon qubits contribute to the secure key is only true for a security proof based on the EDP approach (which is what we use in this paper). It may not be true in other approaches, e.g., the communication complexity approach, as noted in Ref. [43].

The overall gain is given by

$$Q_\mu = \sum_{i=0}^{\infty} Y_i \frac{\mu^i}{i!} e^{-\mu}. \tag{17}$$

The overall QBER is given by

$$E_\mu = \frac{1}{Q_\mu} \sum_{i=0}^{\infty} e_i Y_i \frac{\mu^i}{i!} e^{-\mu}. \tag{18}$$

Without Eve, a normal QKD transmission will give

$$Q_\mu = Y_0 + 1 - e^{-\eta\mu},$$

$$E_\mu Q_\mu = e_0 Y_0 + e_d (1 - e^{-\eta\mu}). \tag{19}$$

B. GLLP idea

We review the idea of GLLP [23] briefly here. GLLP give a security proof of the BB84 QKD when imperfect devices (such as imperfect single-photon sources) are used. There are two kind of qubits discussed by GLLP, tagged and untagged qubits. Tagged qubits are those that have their basis information revealed to Eve, i.e., tagged qubits are not secure for QKD. On the other hand, untagged qubits are secure for QKD. In the BB84 protocol, qubits coming from single-photon states are untagged while those from multiphoton states are tagged because Eve, for instance, can perform PNS attacks [39–42] on the multiphoton states to acquire their basis information. The essential idea of GLLP is that Alice and Bob can apply privacy amplification to tagged and untagged qubits separately. Note that the idea of the tagged state was (perhaps implicitly) introduced in [21].

The data postprocessing of GLLP is performed as follows. First, Alice and Bob apply error correction to all qubits, sacrificing a fraction $H_2(\delta)$ of the key, which is represented in the first term of Eq. (20). Second, in principle, Alice and Bob can distinguish the tagged and untagged qubits, so they can apply the privacy amplification on the tagged and untagged states separately. One can imagine executing privacy amplification on two different strings, the qubits s_{tagged} and $s_{untagged}$ arising from the tagged qubits and the untagged qubits, respectively. Since the privacy amplification is linear (the private key can be computed by applying the C_2 parity check matrix to the qubit string), the key obtained is the bitwise XOR operation

$$s_{untagged} \oplus s_{tagged}$$

of keys that could be obtained from the tagged and untagged qubits separately [23]. If $s_{untagged}$ is private and random, then it does not matter if Eve knows anything about s_{tagged}—the sum will be still private and random. Thus, one needs to apply privacy amplification to the untagged bits alone.

We define the residue of data postprocessing to be the ratio of the final key length to the sifted key length (in an asymptotic sense). The residue of this data postprocessing scheme is given by

$$r_{GLLP} = \max\{- f(\delta) H_2(\delta) + \Omega[1 - H_2(\delta_p)], 0\} \tag{20}$$

where δ is the overall quantum bit error rate, Ω is the fraction of untagged qubits ($\Omega = 1 - \Delta$, where Δ is the fraction of tagged qubits defined by GLLP [23]), δ_p is the phase error rate of the untagged qubits, $f(\cdot)$ is the error correction efficiency as a function of error rate [49], normally $f(x) \geq 1$ with Shannon limit $f(x) = 1$, and $H_2(x)$ is the binary entropy function.

We can further extend GLLP's idea to the case of more than two classes of qubits, i.e., several kinds of qubits with flag g, which generalizes the concept of tagged and untagged qubits. The procedure of data postprocessing is similar: do the overall error correction first and then apply the privacy amplification to each case. So the privacy amplification part can be written as

$$\sum_g \Omega^g H_2(\delta_p{}^g) \tag{21}$$

where one needs to sum over all cases with flag g, Ω_g is the probability of the case with flag g and $\Sigma_g \Omega^g = 1$, and $\delta_p{}^g$ is the phase error rate of the states with flag g. Finally, the residue of data postprocessing is given by

$$r = \max\left\{ - f(\delta) H_2(\delta) + \sum_g \Omega^g [1 - H_2(\delta_p{}^g)], 0 \right\}. \tag{22}$$

Applying the QKD model described in Sec. III A here, $\delta = E_\mu$ and the key generation rate is given by

$$R = q Q_\mu r, \tag{23}$$

where Q_μ and E_μ are the gain and QBER of the signal state, and q is defined similarly as in Eq. (4).

C. Decoy states

For the BB84 protocol, the single-photon state is the only source of final secure keys, i.e., the untagged qubits come from single-photon qubits. So the fraction and error rate of untagged qubit are given by

$$\Omega = Q_1 / Q_\mu, \quad \delta_p = e_1, \tag{24}$$

where Q_1 is given in Eq. (15), e_1 is given by Eq. (16), and Q_μ is given by Eq. (17). By substituting Eq. (20), we can rewrite Eq. (23) into

$$R = q r Q_\mu \geq q\{- Q_\mu f(E_\mu) H_2(E_\mu) + Q_1 [1 - H_2(e_1)]\}, \tag{25}$$

which is given in Eq. (11) of [26].

Q_μ and E_μ can be measured directly from experiment. The question is how to estimate Q_1 and e_1 accurately. In principle, Eve can perform a nondemolition photon-number measurement on the qubits and she may change the yields (Y_i in Sec. III A) of the qubits depending on the measurement outcomes. That is, the yields of qubits, in general, may depend on the photon number. Moreover, Eve can adjust the error rates as she wishes.

The key idea of decoy states is that, instead of just using one coherent state for key transmission, Alice and Bob

choose some decoy states with different expected photon numbers (μ in Sec. III A) to test the channel transmittance and error rate. We emphasize here that decoy states have exactly the same properties other than average photon numbers, so that there is no way for Eve to discriminate between the signal states and decoy states before Alice publicly announce them. Consequently, we have $Y_i(\text{decoy}) = Y_i(\text{signal})$ and $e_i(\text{decoy}) = e_i(\text{signal})$.

Specifically, the overall gain and the overall QBER in Eqs. (17) and (18) can be estimated for a fixed μ in the experiment by Alice and Bob. By changing μ over many values, a set of linear equations in the form of Eqs. (17) and (18) with unknowns Y_i and e_i are obtained. Thus, Alice and Bob can easily solve for Y_i and e_i from these equations. For the BB84 protocol, they are interested only in Y_1 and e_1. With the decoy state, Alice and Bob can estimate the yields and error rates of single-photon states (Y_1 and e_1) accurately.

Here we will briefly review the results of decoy-state protocols. Details can be seen in [26,27]. In the *asymptotic* decoy-state case [26], we assume that infinite decoy states are employed by Alice and Bob, so they can solve the infinite number of linear equations in the form of Eqs. (17) and (18) to get all values of $\{Y_i\}$ and $\{e_i\}$ accurately. In the simulation, we will simply take the values of Eq. (14) and (16) directly.

In the *practical* case, Alice and Bob need to use only two decoy states, a vacuum and weak decoy state. Then they can bound Y_1 and e_1 by [Eqs. (34) and (37) in [27]]

$$Y_1 \geq \frac{\mu}{\mu\nu - \nu^2}\left(Q_\nu e^\nu - Q_\mu e^\mu \frac{\nu^2}{\mu^2} - \frac{\mu^2 - \nu^2}{\mu^2}Y_0\right), \quad (26)$$

$$e_1 \leq \frac{E_\nu Q_\nu e^\nu - e_0 Y_0}{Y_1 \nu},$$

where ν is the expected photon number of the weak decoy state. We remark that when $\nu \to 0$, Eqs. (26) will asymptotically approach Eqs. (14) and (16).

IV. BOUNDS

In QKD experiments, we are interested in maximizing three quantities—the tolerable error rates, the key generation rate, and the maximal secure distance. In this section, we will give these three bounds due to the QKD setup model discussed in Sec. III A.

A. Bounds of error rates

Here, we will consider the bounds of error rates (bit error rate δ_b and phase error rate δ_p), assuming a laser source that emits a fixed number of photons in each pulse (e.g., a basis-dependent single-photon source). The upper bounds can be derived by considering some simple attacks (such as the intercept-resend attack) and determining the QBER caused by these attacks. The lower bounds can be determined by the unconditional security proof assuming that Eve is performing an arbitrary attack allowed by the law of quantum mechanics and Alice and Bob employ some special data postprocessing schemes (such as the Gottesman-Lo EDP described in Sec.

II A). One lower bound, obtained by considering the Gottesman-Lo EDP, is 18.9% [8]. For the BB84 protocol, an upper bound, obtained by considering an intercept-resend attack, is 25%.

Here, we consider the lower bound in a general setting where the error rates are characterized by (δ_b, δ_p). In general, the bit error rate δ_b can be measured by error testing, but the phase error rate δ_p cannot be directly observed from the QKD experiment. In order to guarantee security, Alice and Bob have to bound δ_p with the knowledge of δ_b. For the BB84 protocol with an ideal single-photon source, due to the symmetry between the X and Z bases, one can show that the bit error rate and the phase error rate are the same, i.e.,

$$\delta_b = \delta_p. \quad (27)$$

In general, for other protocols or with nonideal sources (including coherent sources), the bit and phase error rates are different. For example, even for the BB84 protocol, when a basis-dependent source is used, Eq. (27) may not hold. In this case, according to Eq. (9) of [34], due to the concavity of the right-hand side of the equation, it is not hard to show (see Appendix B) that δ_b and δ_p have the relation

$$\sqrt{F} \leq \sqrt{(1 - \delta_b)(1 - \delta_p)} + \sqrt{\delta_b \delta_p}, \quad (28)$$

where F is the fidelity between the two states with two bases (X and Z) sent by Alice, and it is the single parameter that characterizes the basis dependency of the source. Thus, Alice and Bob can upper bound δ_p (denoted as δ_p^u) with this inequality, given δ_b. Clearly, when $\delta_p = \delta_b$, the inequality will always be satisfied, i.e., $\delta_p = \delta_b$ is a particular solution of Eq. (28). Therefore, in general we have $\delta_p^u \geq \delta_p$. In the following, we use δ_p to denote the upper bound δ_p^u for simplicity.

Given a QKD protocol and a laser source, Alice and Bob can estimate the phase error rate δ_p from the bit error rate δ_b according to the protocol and the source. We investigate the highest error rates that a data postprocessing scheme can tolerate. Figure 2 shows the tolerable error rates of the Gottesman-Lo EDP compared to the 1-LOCC EDP scheme, illustrating the superior performance of the Gottesman-Lo EDP over the 1-LOCC EDP. The boundaries of error rates are found by searching through the regime of

$$\delta_b \leq \delta_p, \quad \delta_b + \delta_p < 1/2 \quad (29)$$

such that positive key rates are obtained. The reason we are interested in the region specified by the second inequality in Eq. (29) is as follows. We can assume that the error rates δ_b and δ_p are less than $1/2$, otherwise Alice and Bob can flip the qubits. Also, if $\delta_b + \delta_p \geq 1/2$, then all the diagonal elements of the density matrix in Eq. (1) that Alice and Bob share are no greater than $1/2$ (by setting $q_{11} = 0$). Thus, the diagonalized density matrix is separable [32] and the Gottesman-Lo EDP cannot distill any pure EPR pairs.

The input to the Gottesman-Lo EDP is $(q_{00}, q_{10}, q_{11}, q_{01})$ with $q_{00} + q_{10} + q_{11} + q_{01} = 1$ (see Sec. II A). But Alice and Bob only know $\delta_b = q_{10} + q_{11}$ and $\delta_p = q_{11} + q_{01}$ from their error test. There is one free parameter q_{11}. In Appendix C of [8], the authors have proved that $q_{11} = 0$ is the worst case when $\delta_b = \delta_p$. Following that proof, we can show that $q_{11} = 0$ is the worst case when the condition of Eq. (29) is satisfied. That
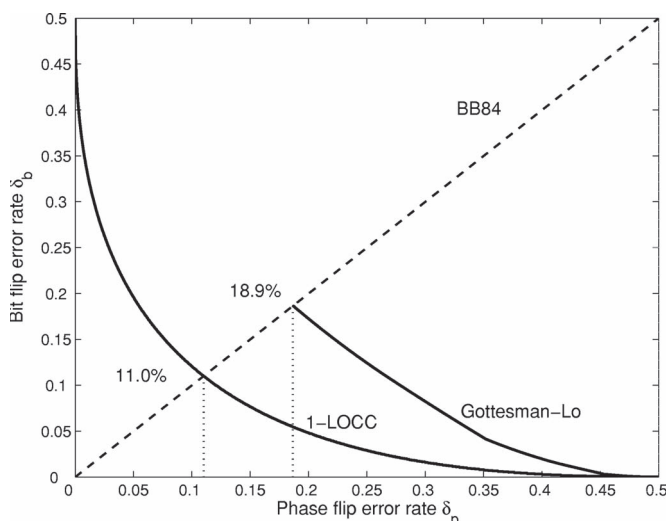
FIG. 2. Plot of the secure regions in terms of error rates for 1-LOCC and Gottesman-Lo EDPs. The regions under the solid lines are proven to be secure due to 1-LOCC EDP, and Gottesman-Lo EDP schemes (for the region under the solid line and dashed line), respectively. For the 1-LOCC EDP, we use Eq. (4). For the Gottesman-Lo EDP, we use Eqs. (6) and (8). In the Gottesman-Lo EDP, we optimize the B-P sequence up to 12 steps.

is, given (δ_b, δ_p), if we check the input $(1 - \delta_b - \delta_p, \delta_b, 0, \delta_p)$ for the Gottesman-Lo EDP and get a positive key rate, then we can safely claim that the Gottesman-Lo EDP can tolerate the error rates of (δ_b, δ_p).

To determine the tolerable bit error rate of a particular protocol, one should first obtain the relationship between the bit error rate and the phase error rate, and plot it in Fig. 2. The intersections between this curve and the boundary curves (the 1-LOCC and the Gottesman-Lo curves) indicate the tolerable QBER for the corresponding EDPs. For example, for the BB84 protocol with a perfect single-photon source, we have $\delta_b = \delta_p$, which is the dashed line plotted in Fig. 2. We can immediately read off from the figure that an initial bit error rate of 18.9% is tolerable using the Gottesman-Lo EDP [8], while an error rate of 11.0% is tolerable using the 1-LOCC EDP. In general, the Gottesman-Lo EDP gives rise to higher tolerable error rates than does the 1-LOCC EDP.

For protocols having constraints on q_{11}, such as the six-state protocol [46] and the SARG04 protocol with a single-photon source [43,47,48], the tolerable QBER can go beyond the boundary curves shown in Fig. 2.

We wrote a computer program to exhaustively search for the optimal B-P sequence up to 12 steps. The precision of the program is 10^{-15}.

B. Distance upper bound

Let us come back to the realistic QKD setup model discussed in Sec. III A. An upper bound on the bit error rate of the single-photon state is 25%, above which the BB84 protocol is broken by the intercept-resend attack. The maximal secure distance then can be bounded by the distance when

the bit error rate of the single-photon state reaches 25%.

The error rate of the single-photon state e_1 is given in Eq. (16),

$$e_1 = \frac{e_d \eta + \frac{1}{2} Y_0}{\eta + Y_0},$$

where e_d is the intrinsic error rate of the detector in Bob's side, η is the overall transmittance, and Y_0 is the background rate. Thus, e_1 exceeds 25% when

$$\eta \leqslant \frac{0.25 Y_0}{0.25 - e_d}. \tag{30}$$

In the case of GYS [19], the fiber loss is $\alpha = 0.21$ dB/km, $e_d = 3.3\%$, and $Y_0 = 1.7 \times 10^{-6}$; then the upper bound of secure distance is 208 km.

C. Key generation rate upper bound

According to our model, the final secure key can be derived only from single-photon qubits. To derive the upper bound of the key generation rate, we assume that Alice and Bob can distinguish the single-photon qubits from other qubits (vacuum and multiphoton qubits). So they can perform the classical data postprocessing only on to the single-photon qubits. One upper bound of key generation rate is given by the *mutual information* between Alice and Bob [50],

$$R^U = Q_1[1 - H_2(e_1)], \tag{31}$$

where Q_1 is the yields of single-photon states and e_1 is the error rate of single-photon states.

Note that the above two upper bounds, Eqs. (30) and (31), assume that (a) Alice and Bob cannot distinguish background counts and true signal counts and (b) a secure key can only be extracted from the single-photon states. Also, these two bounds are general upper bounds regardless of the technique used for combating the effect of imperfect devices such as the decoy-state technique.

V. DECOY+GLLP+GOTTESMAN-LO EDP

In this section, we propose a 2-LOCC-based data postprocessing protocol with the form of a sequence of B steps, followed by error correction and privacy amplification, as discussed in Sec. II A. This scheme is a generalization of the Gottesman-Lo scheme to the case of imperfect devices. The reasons why we skip P steps here are as follows. First, from the simulation in Sec. IV A, we found that P steps are not as useful as B steps. Second, considering only B steps can simplify the procedure of the data postprocessing scheme. The procedure of this data postprocessing is as follows:

(1) Alice and Bob perform a sequence of B steps to the sifted keys [corresponding to $\tilde{r}_B$ in Eq. (32)].

(2) They calculate the variables (such as QBER, untagged qubit ratio) after the B steps.

(3) They perform overall error correction [corresponding to the first term in Eq. (32)].

(4) They perform privacy amplification [corresponding to the second term in Eq. (32)].

In the following, we will discuss how to calculate the residue of this data postprocessing scheme.

In the decoy protocol, there are three kind of qubits: vacuum, single-photon, and multiphoton qubits, described in Sec. III A. We emphasize again here that the final secure key can only be distilled from untagged qubits (single-photon qubits).

Since either of the two inputs of a B step has three possibilities, the outcomes of a B step then have nine possibilities. Only the case where both inputs are untagged qubits has a positive contribution to the final secure key and all other privacy amplification terms in Eq. (22) will be zero. That is, at the end of some B steps and bit error correction, privacy amplification can be applied only to the remaining qubits that come from the case where both inputs are untagged qubits. In other words, an output qubit after a subsequence of B steps is "untagged" if and only if (a) it passes all B steps and (b) it is generated from the case where all initial input qubits are single photon-qubits. Therefore, the residue ratio of data postprocessing can be expressed, according to Eq. (22), as

$$r = \max(\tilde{r}_B\{-f(\tilde{\delta})H_2(\tilde{\delta}) + \tilde{\Omega}[1 - H_2(\tilde{\delta}_p^{untagged})]\}, 0) \quad (32)$$

where $\tilde{\delta}$ is the overall QBER, $\tilde{r}_B$ is the overall survival residue, $\tilde{\Omega}$ is the fraction of untagged states in the final survival states, and $\tilde{\delta}_p^{untagged}$ is the phase error rate of the untagged states, after a sequence of B steps. In the following, we will show how these variables change on performing B steps.

An arbitrary B step

Let us consider how the various quantities (fraction of untagged states Ω, QBER of overall surviving states δ, bit error rate $\delta_{untagged}$, and phase error rates δ_p of the untagged states) are transformed under one step in a B step sequence.

Before a B step, the fraction of untagged states is Ω, the overall QBER is δ, the bit error rate of the untagged states is $\delta_{untagged}$, and the phase error rate of the untagged states is δ_p. According to Eq. (5) the overall survival probability p_S and the survival probability of the untagged states $p_S^{untagged}$ after one B step are given by

$$p_S = [\delta^2 + (1 - \delta)^2],$$

$$p_S^{untagged} = [\delta_{untagged}^2 + (1 - \delta_{untagged})^2]. \quad (33)$$

Then the residue after one B step is given by

$$r_B = \frac{1}{2}p_S. \quad (34)$$

The factor $\frac{1}{2}$ in Eq. (34) due to the fact that Alice and Bob keep only one qubit from a survival pair. Then, after a B step the fraction of untagged states Ω' is given by

$$\Omega' = \frac{\Omega^2 p_S^{untagged}}{p_S}. \quad (35)$$

The change of overall QBER δ' is given by

Wavelength (nm)	α (dB/km)	η_{Bob}	e_d	Y_0
1550	0.21	4.5%	3.3%	1.7×10^{-6}

$$\delta' = \frac{\delta^2}{\delta^2 + (1 - \delta)^2}. \quad (36)$$

Before the first round of B step, the initial density matrix of untagged state is $(1 - 2e_1 + q_{11}, e_1 - q_{11}, q_{11}, e_1 - q_{11})$, where e_1 is the error rate of single-photon states. From Appendix C of [8], we know that $q_{11} = 0$ is the worst case for B steps. Thus we can conservatively choose $(1 - 2e_1, e_1, 0, e_1)$ as the initial input density matrix. If only B steps are performed, $q_{11} = 0$ will always be satisfied, according to Eq. (6). So the input untagged qubits for any round of B steps has the form of

$$(q_{00}, q_{10}, q_{11}, q_{01}) = (1 - \delta_{untagged} - \delta_p, \delta_{untagged}, 0, \delta_p). \quad (37)$$

The bit error rate of untagged states $\delta'_{untagged}$ depends only on the input $\delta_{untagged}$,

$$\delta'_{untagged} = \frac{\delta_{untagged}^2}{\delta_{untagged}^2 + (1 - \delta_{untagged})^2}. \quad (38)$$

According to Eqs. (6), (7), and (37), the phase error rate of untagged states is

$$\delta'_p = q'_{11} + q'_{01} = \frac{2q_{10}q_{11} + 2q_{00}q_{01}}{(q_{10} + q_{11})^2 + (q_{00} + q_{01})^2}$$
$$= \frac{2\delta_p(1 - \delta_{untagged} - \delta_p)}{\delta_{untagged}^2 + (1 - \delta_{untagged})^2}. \quad (39)$$

Equations (33)–(39) are valid for a general B step. Alice and Bob can perform a sequence of B steps as described above and then do the error correction and privacy amplification. Once all these quantities are obtained, the key generation rate can be calculated from Eq. (32).

To illustrate the improvement made by introducing B steps, we numerically calculated the key generation rate assuming the parameters in the GYS experiment [19]. Note that the overall QBER $\tilde{\delta}$ in Eq. (32) never exceeds 10%. The value of $f(e) = 1.22$ is the upper bound according to [49]. The parameters used for simulation are listed in Table I.

From Fig. 3, we can see that there is a nontrivial extension of the maximal secure distance after introducing B steps. We remark that the key generation rate decoy-state protocol with one B step is higher than the one with 1-LOCC from the distance around 132 km. The maximal secure distance using four B steps is 181 km, which is not far from the upper bound of 208 km given in Sec. IV B. Even with only one B step, the maximal secure distance can be extended from 142 to 162 km. Thus, B steps are very useful in QKD data postprocessing.
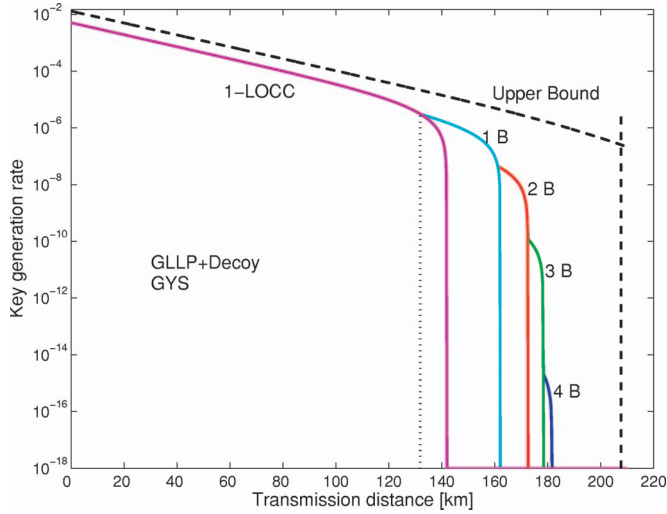
FIG. 3. (Color online) Plot of the key generation rate as a function of the transmission distance with the data postprocessing scheme of GLLP+decoy+B steps method. The parameters used are from the GYS experiment [19] listed in Table I. The GLLP +decoy+B steps scheme surpasses the scheme with 1-LOCC at a distance of 132 km. The maximal secure distance using four B steps is 181 km, which is not far from the upper bound of 208 km.

VI. DECOY+GLLP+RECURRENCE EDP

In this section, we propose a second 2-LOCC-based data postprocessing scheme based on the recurrence scheme [10], which is reviewed in Sec. II B. Our scheme is a generalization of the recurrence scheme to the case of imperfect sources.

In Sec. III B, we give a formula, Eq. (22), for the key generation rate using the idea of GLLP. Let us combine recurrence with Eq. (22). So, instead of just taking care of one kind of qubit, we need to apply privacy amplification to several groups of qubits separately, i.e., we will have several K_i in Eq. (A6). After the recurrence, the data postprocessing residue rate becomes

$$r = -\frac{1}{2}f(p_S)H_2(p_S) - \frac{1}{2}p_Sf\left(\frac{\delta^2}{p_S}\right)H_2\left(\frac{\delta^2}{p_S}\right) + \sum_i \Omega_i K_i,$$

(40)

where p_S is the even-parity possibility given in Eq. (A2) with $\delta_b^C = \delta_b^T = \delta$, δ is the overall QBER before the recurrence, $f(\cdot)$ is the error correction efficiency, and Ω_i and K_i are the probability and the residue of the qubit groups with label i after privacy amplification, respectively. Here, Alice and Bob first check the parity corresponding to the first term of Eq. (40). Second, they apply overall error correction to the qubits with even parity, corresponding to the second term of Eq. (40). Third, they measure one of the qubits in those pairs with odd parity to obtain the error syndrome of another qubit. Afterward, they can group the surviving qubits into several groups with labels i. Finally, they perform privacy amplification on each group with label i, corresponding to the last term of Eq. (40).

TABLE II. Input parameters of three kinds of qubits for recurrence. Following Eqs. (15) and (17), the fractions of each group are given by $\Omega_V = Q_0/Q_\mu$, $\Omega = Q_1/Q_\mu$, and $\Omega_M = 1 - \Omega_V - \Omega$. $\Omega_V/2 + e_1\Omega + e_M\Omega_M = \delta$ is the overall QBER.

Qubit	Fraction	δ_b	δ_p	q_{11}
V	Ω_V	$1/2$	$1/2$	q_{11}^V
S	Ω	e_1	e_1	a
M	Ω_M	e_M	$1/2$	q_{11}^M

Consider the decoy-state case, Alice and Bob have three kinds of input qubits: vacuum qubits (V), single-photon qubit (S), and multiphoton qubits (M). The input parameters for recurrence are listed in Table II.

Thus, the outcome of one round of recurrence will have nine cases. Clearly, if neither input is a single-photon qubit, the outcome will have no contribution to the final key. Alice and Bob need only apply Eq. (A12) to calculate the residues K_i for the five cases: $V \otimes S$, $S \otimes V$, $S \otimes S$, $S \otimes M$, $M \otimes S$. The probabilities of occurrence, Ω_i, for the five cases are, respectively, $\Omega_V\Omega$, $\Omega\Omega_V$, Ω^2, $\Omega\Omega_M$, and $\Omega_M\Omega$. Once we know K_i and Ω_i, we can then determine the overall residue r using Eq. (40) (details are shown in Appendix C):

$$r \geq -B + C - F_a$$

(41)

where

$$B = \frac{1}{2}f(p_S)H_2(p_S) + \frac{1}{2}p_Sf\left(\frac{\delta^2}{p_S}\right)H_2\left(\frac{\delta^2}{p_S}\right),$$

$$C = \frac{3}{4}\Omega_V\Omega + \Omega^2(1 - e_1 + e_1^2) + \frac{1}{2}\Omega\Omega_M(2 - e_1 - e_M + 2e_1e_M),$$

$$D_1 = \frac{3}{4}\Omega_V\Omega + \frac{1}{2}\Omega^2(2 - e_1) + \frac{1}{2}\Omega\Omega_M(2 - e_M),$$

$$D_2 = \frac{3}{4}\Omega_V\Omega + \frac{1}{2}\Omega^2(1 + e_1) + \frac{1}{2}\Omega\Omega_M(e_M + 1),$$

$$F_a = D_1(1 - e_1)H_2\left(\frac{e_1 - a}{1 - e_1}\right) + D_2e_1H_2\left(\frac{a}{e_1}\right),$$

(42)

with equality when $q_{11}^V = 1/4$ and $q_{11}^M = e_M/2$. In order to get a lower bound of the key generation rate R, we maximize F_a over a by using a bisection method as discussed in Appendix C.

Figure 4 shows the key generation rate as a function of the transmission distance for the GLLP+decoy+1-LOCC, GLLP+decoy+one B step, and GLLP+decoy+recurrence methods. Recurrence does have some improvement (more than 10%) in the key generation rate over 1-LOCC for short distances, and it also increases the maximal secure distance by 6 km. We remark that recurrence is useful even in the short-distance regime.
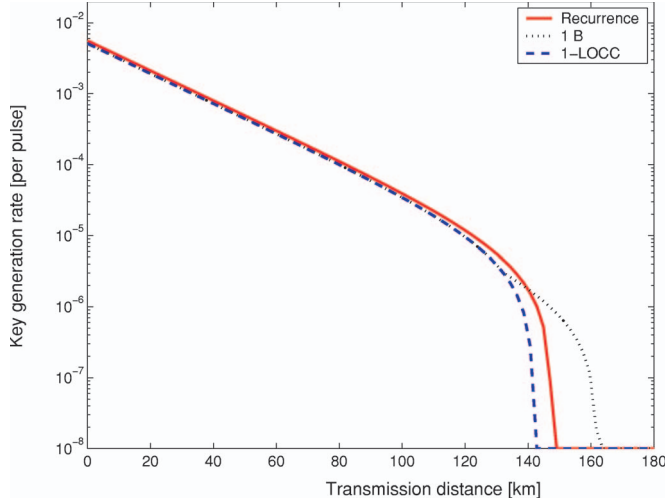
FIG. 4. (Color online) Plot of the key generation rate as a function of the transmission distance, GLLP+decoy+recurrence method vs GLLP+decoy+1-LOCC method. Recurrence does have some improvement over 1-LOCC in the whole regime of distances. In particular, the recurrence method increases the key generation rate by more than 10% in our simulation. The maximal secure distance for each case is 142.8 km (1-LOCC), 149.1 km (recurrence), and 163.8 km (one B step), respectively. Here we consider the asymptotic decoy-state QKD case with infinitely long signals. The parameters used are from the GYS experiment [19] listed in Table I.

VII. STATISTICAL FLUCTUATIONS

In a realistic QKD experiment, only a finite number of signals are transmitted. Thus, the estimations of Y_1 and e_1 have certain statistical fluctuations. These statistical fluctuations in decoy-state QKD with 1-LOCC are analyzed in [27] and also [28]. In this section, we will consider statistical fluctuations for the two data postprocessing schemes with 2-LOCC discussed in Secs. V and VI.

As pointed out in [27], considering statistical fluctuations of QKD is a hard problem. Here we will follow the standard error analysis technique to analyze statistical fluctuations as used in [27]. We can incorporate statistical fluctuations in the two 2-LOCC data postprocessing schemes decoy+GLLP +B steps and decoy+GLLP+recurrence.

In [27], Q_1 and e_1 are bounded when taking statistical fluctuations into account. As for the postprocessing with 2-LOCC described in Sec. V, the inputs of the B steps are Q_μ and E_μ, which can be measured directly from experiment, and Q_1 and e_1, which are estimated by the decoy method. Evidently, one should take the lower bound of Q_1 and the upper bound of e_1 to lower bound the key rate R. Thus the procedure will be as follows: first, with the decoy method, one can lower bound Q_1 and upper bound e_1, and then input the four parameters (Q_μ, E_μ, Q_1, and e_1) into the data postprocessing of the GLLP+decoy+B step method to extract secure keys.

As for the case of recurrence, from Table II, Alice and Bob have to estimate Q_0 besides the four parameters discussed above. From Eq. (41), it is not clear which bounds of Q_0 one should pick up to lower bound the key rate. One can clearly see that lower bounding Eq. (41) is a hard problem.
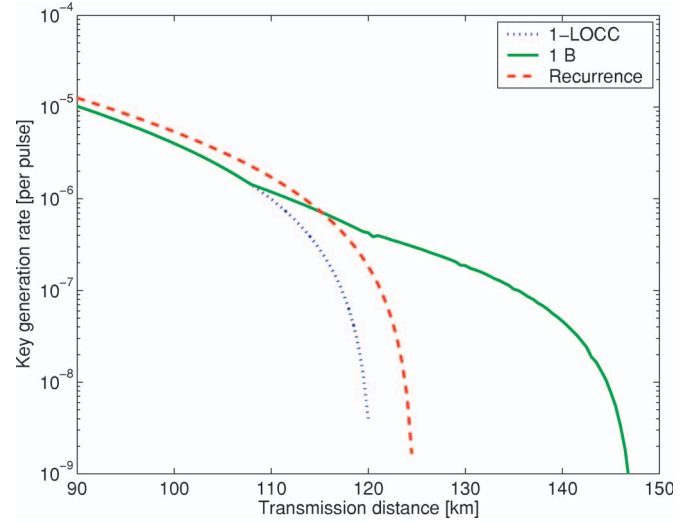

FIG. 5. (Color online) Plot of the simulation results for three data postprocessing schemes of the decoy-state protocol, decoy+1 -LOCC, decoy+one B step, and decoy+recurrence, considering statistical fluctuations. The maximal secure distances of three schemes are 120, 125, and 147 km, respectively. The parameters used are from the GYS experiment [19] listed in Table I.

Instead of going to tedious mathematical calculations here, we have a plausible argument based on our physical intuition. First of all, single-photon qubits are "good" qubits in our discussion. So we reasonably assume that Alice and Bob can safely use the lower bound of Q_1 and the upper bound of e_1 to lower bound the key rate. As discussed in [51], the vacuum decoy state can have positive contribution in the privacy amplification procedure. Also, in the Appendix of [27], we proved that one should take the lower bound of Y_0 to lower bound the key generation rate in the 1-LOCC case. Thus, here we take the lower bound of Q_0 to estimate the key rate.

The results are shown in Fig. 5. Here, we assume that Alice and Bob use 6×10^9 pulses. These pulses are randomly selected as signal and decoy states. The distribution among the signal states, vacuum states, and weak decoy states was found by an exhaustive search for the optimal one. Then, we use ten standard deviations to bound Q_ν, E_ν, and Y_0, and substitute the worst-case values of these into

$$Q_1 \geqslant Q_1^{L,\nu,0} = \frac{\mu^2 e^{-\mu}}{\mu\nu - \nu^2}\left(Q_\nu e^\nu - Q_\mu e^\mu \frac{\nu^2}{\mu^2} - \frac{\mu^2 - \nu^2}{\mu^2}Y_0\right),$$

$$e_1 \leqslant e_1^{U,\nu,0} = \frac{E_\nu Q_\nu e^\nu - e_0 Y_0}{Y_1^{L,\nu,0}\nu} \qquad (43)$$

to bound Q_1 and e_1. Here, ν is the expected photon number of the weak decoy states, and Q_ν and E_ν are the gain and QBER of the weak decoy states. We can see that with statistical fluctuations, the improvements of 2-LOCC are still notable.

VIII. CONCLUSION

We have developed two data postprocessing schemes for decoy-state QKD using 2-LOCC, one based on B steps and the other based on the recurrence method. The distance of secure QKD is crucial in practical applications. Therefore, our decoy+B steps postprocessing protocol, which we have shown to be able to increase the maximal secure distance of QKD from about 141 to about 182 km (using parameters from the GYS experiment [19]), proves to be useful in real-life applications. Moreover, our work shows that recurrence protocols are useful for increasing the key generation rate in a practical QKD system in the whole regime of distances. While we have focused our modeling on a fiber-based QKD system, our general formalism applies also to open-air QKD systems.

We have shown that similar conclusions hold even with statistical fluctuations in the experimental variables for the decoy+B step scheme. For the decoy+recurrence scheme, although we do not have a rigorous argument, physical intuition suggests that similar conclusions hold in the case of considering statistical fluctuations as well. We conclude that using two-way classical communication is superior to using one-way for our decoy-state QKD schemes.

In addition, we provided the region of bit error rates and phase error rates that are tolerable by using the Gottesman-Lo EDP scheme. Also, we calculated the upper bounds on distance and on the key generation rate of a real QKD setup based on our model.

APPENDIX A: KEY RATE OF THE RECURRENCE SCHEME WITH AN IDEAL SOURCE

In this section, we review the recurrence EDP and develop the key generation rate formula given by

$$R = qr, \tag{A1}$$

where q depends on the implementation of the QKD ($1/2$ for the BB84 protocol, because half the time the Alice and Bob bases are not compatible) and r is the residue, which we will find in the following. We use the same notation as in Sec. II and consider a Bell diagonal state $(q_{00}, q_{10}, q_{11}, q_{01})$.

1. Parity check

As the first step of recurrence, Alice and Bob check the parity of two pairs (labeled as the control qubit C and target qubit T). They will get even parity if the two pairs are in one of the states

$$0000, 0001, 0100, 0101, 1010, 1011, 1110, 1111,$$

and will get odd parity if they are in one of the states

$$0010, 0011, 0110, 0111, 1000, 1001, 1100, 1101,$$

where the first two bits represent the control qubit, and the last two bits represent the target qubit. That is, ij represents the Bell state $|\psi_{ij}\rangle$ as given in Eq. (2) with $i, j = 0, 1$. For example, 1110 means that there is a bit error and a phase error in the control qubit ($|\psi_{11}\rangle$), and a bit error and no phase error in the target qubit ($|\psi_{10}\rangle$). Thus, the probability to get even parity is given by

$$
\begin{aligned}
p_S &= (q_{00}^C + q_{01}^C)(q_{00}^T + q_{01}^T) + (q_{10}^C + q_{11}^C)(q_{10}^T + q_{11}^T) \\
&= (1 - \delta_b^C)(1 - \delta_b^T) + \delta_b^C \delta_b^T, \tag{A2}
\end{aligned}
$$

where $\delta_b^C = q_{10}^C + q_{11}^C$ and $\delta_b^T = q_{10}^T + q_{11}^T$ are the bit error rates of the input control and target qubits, respectively. During the parity check, the number of pure EPR pairs (or secret bits) that Alice and Bob need to sacrifice is given by

$$\frac{1}{2}H_2(p_S), \tag{A3}$$

where $\frac{1}{2}$ is due to the fact that Alice and Bob compute the parity of two-qubit pairs at one time.

After the parity check, the qubits are divided into two groups, qubits with even parity and those with odd parity. In the following, we will discuss the error correction and privacy amplification of these two groups separately. The recurrence protocol appearing in [10] only performs error correction on qubits with even parity.

2. Error correction

For even-parity qubits, we can see that the bit error syndrome of control qubits will be the same as that of target qubits. Thus, Alice and Bob need to do error correction on only the control (or target) qubits. According to Eq. (7), the bit error rate of control qubits after recurrence is given by

$$\widetilde{\delta}_b^C = \frac{(q_{10}^C + q_{11}^C)(q_{10}^T + q_{11}^T)}{p_S} = \frac{\delta_b^C \delta_b^T}{p_S} \tag{A4}$$

where p_S is the probability of even parity in the recurrence given by Eq. (A2). Therefore, Alice and Bob need to sacrifice a fraction

$$\frac{1}{2}p_S H_2(\widetilde{\delta}_b^C) = \frac{1}{2}p_S H_2\left(\frac{\delta_b^C \delta_b^T}{p_S}\right) \tag{A5}$$

to do the overall error correction. The factor $\frac{1}{2}$ is due to the fact that control qubits have the same error syndrome as target qubits.

Therefore the residue of data postprocessing, similar to Eq. (20), can be expressed as

$$r = -\frac{1}{2}H_2(p_S) - \frac{1}{2}p_S H_2\left(\frac{\delta_b^C \delta_b^T}{p_S}\right) + K \tag{A6}$$

where p_S is given in Eq. (A2) and K is the residue of privacy amplification, which we will focus on in the following.

3. Privacy amplification

Alice and Bob perform privacy amplification to the qubits with even and odd parity separately.

a. Even parity

Now, Alice and Bob already know the bit error syndrome. The control and target qubits have the same bit error syndromes, but may have different phase error syndromes. Thus, Alice and Bob can divide the even-parity qubits into four groups: control qubits with bit error syndrome 0 and 1, and target qubits with bit error syndrome 0 and 1, and treat these groups separately in the privacy amplification step. The probability of each group [summing together the even-parity probabilities given in Eq. (A2)] is given by

$$\frac{(q_{00}^C + q_{01}^C)(q_{00}^T + q_{01}^T)}{2}, \quad \frac{(q_{10}^C + q_{11}^C)(q_{10}^T + q_{11}^T)}{2},$$

$$\frac{(q_{00}^C + q_{01}^C)(q_{00}^T + q_{01}^T)}{2}, \quad \frac{(q_{10}^C + q_{11}^C)(q_{10}^T + q_{11}^T)}{2}$$

with phase error rate

$$\frac{q_{01}^C}{q_{00}^C + q_{01}^C}, \quad \frac{q_{11}^C}{q_{10}^C + q_{11}^C}, \quad \frac{q_{01}^T}{q_{00}^T + q_{01}^T}, \quad \frac{q_{11}^T}{q_{10}^T + q_{11}^T}.$$

Since the error syndrome of each group of qubits is known to Alice and Bob, privacy amplification can be applied to the different groups separately. Then, Alice and Bob should sacrifice a fraction

$$\frac{(q_{00}^C + q_{01}^C)(q_{00}^T + q_{01}^T)}{2} H_2\left(\frac{q_{01}^C}{q_{00}^C + q_{01}^C}\right)$$

$$+ \frac{(q_{10}^C + q_{11}^C)(q_{10}^T + q_{11}^T)}{2} H_2\left(\frac{q_{11}^C}{q_{10}^C + q_{11}^C}\right)$$

$$+ \frac{(q_{00}^C + q_{01}^C)(q_{00}^T + q_{01}^T)}{2} H_2\left(\frac{q_{01}^T}{q_{00}^T + q_{01}^T}\right)$$

$$+ \frac{(q_{10}^C + q_{11}^C)(q_{10}^T + q_{11}^T)}{2} H_2\left(\frac{q_{11}^T}{q_{10}^T + q_{11}^T}\right) \quad \text{(A7)}$$

to do the privacy amplification. Given the bit and phase error rates of input control and target qubits $\delta_p^C = q_{11}^C + q_{01}^C$ and $\delta_p^T = q_{11}^T + q_{01}^T$, Eq. (A7) can be written as

$$\frac{1}{2}(1 - \delta_b^C)(1 - \delta_b^T)\left[H_2\left(\frac{\delta_p^C - q_{11}^C}{1 - \delta_b^C}\right) + H_2\left(\frac{\delta_p^T - q_{11}^T}{1 - \delta_b^T}\right)\right]$$

$$+ \frac{1}{2}\delta_b^C \delta_b^T\left[H_2\left(\frac{q_{11}^C}{\delta_b^C}\right) + H_2\left(\frac{q_{11}^T}{\delta_b^T}\right)\right]. \quad \text{(A8)}$$

Thus the privacy amplification residue of even-parity qubits is given by

$$K_{even} = p_S - \frac{1}{2}(1 - \delta_b^C)(1 - \delta_b^T)\left[H_2\left(\frac{\delta_p^C - q_{11}^C}{1 - \delta_b^C}\right)\right.$$

$$\left. + H_2\left(\frac{\delta_p^T - q_{11}^T}{1 - \delta_b^T}\right)\right] - \frac{1}{2}\delta_b^C \delta_b^T\left[H_2\left(\frac{q_{11}^C}{\delta_b^C}\right) + H_2\left(\frac{q_{11}^T}{\delta_b^T}\right)\right].$$

$$\text{(A9)}$$

b. Odd parity

It turns out that pairs with odd parity during the recurrence can also contribute to the final key [10]. Instead of including them in the error correction, Alice and Bob measure one of the two qubits and hence they know the bit error syndrome of the remaining qubit. They can then proceed with privacy amplification on those qubits.

Suppose Alice and Bob always choose to measure the target qubits and obtain the error syndrome of the control qubits. Similarly to the even-parity case, now, Alice and Bob can divide the control qubits with odd parity into two parts according to the bit error syndrome. The probability of each part is given by

$$\frac{(q_{00}^C + q_{01}^C)(q_{10}^T + q_{11}^T)}{2}, \quad \frac{(q_{10}^C + q_{11}^C)(q_{00}^T + q_{01}^T)}{2},$$

with phase error rate

$$\frac{q_{01}^C}{q_{00}^C + q_{01}^C}, \quad \frac{q_{11}^C}{q_{10}^C + q_{11}^C}.$$

With the same argument as Eq. (A7), the number of qubits that need be sacrificed for privacy amplification is given by

$$\frac{(q_{00}^C + q_{01}^C)(q_{10}^T + q_{11}^T)}{2} H_2\left(\frac{q_{01}^C}{q_{00}^C + q_{01}^C}\right)$$

$$+ \frac{(q_{10}^C + q_{11}^C)(q_{00}^T + q_{01}^T)}{2} H_2\left(\frac{q_{11}^C}{q_{10}^C + q_{11}^C}\right)$$

$$= \frac{1}{2}\left[(1 - \delta_b^C)\delta_b^T H_2\left(\frac{\delta_p^C - q_{11}^C}{1 - \delta_b^C}\right) + \delta_b^C(1 - \delta_b^T)H_2\left(\frac{q_{11}^C}{\delta_b^C}\right)\right].$$

$$\text{(A10)}$$

So the privacy amplification residue of odd-parity qubits is given by

$$K_{odd} = \frac{1}{2}(1 - \delta_b^C)\delta_b^T\left[1 - H_2\left(\frac{\delta_p^C - q_{11}^C}{1 - \delta_b^C}\right)\right]$$

$$+ \frac{1}{2}\delta_b^C(1 - \delta_b^T)\left[1 - H_2\left(\frac{q_{11}^C}{\delta_b^C}\right)\right]. \quad \text{(A11)}$$

Therefore, the privacy amplification residue K in Eq. (A6), by adding Eq. (A9) and Eq. (A11) and substituting Eq. (A2), is given by

$$K = K_{even} + K_{odd} = 1 - \frac{1}{2}(1 - \delta_b^C)\delta_b^T - \frac{1}{2}\delta_b^C(1 - \delta_b^T)$$

$$- \frac{1}{2}(1 - \delta_b^C)H_2\left(\frac{\delta_p^C - q_{11}^C}{1 - \delta_b^C}\right) - \frac{1}{2}\delta_b^C H_2\left(\frac{q_{11}^C}{\delta_b^C}\right)$$

$$- \frac{1}{2}(1 - \delta_b^C)(1 - \delta_b^T)H_2\left(\frac{\delta_p^T - q_{11}^T}{1 - \delta_b^T}\right)$$

$$- \frac{1}{2}\delta_b^C \delta_b^T H_2\left(\frac{q_{11}^T}{\delta_b^T}\right). \quad \text{(A12)}$$

Note that there are two free parameters q_{11}^C and q_{11}^T in Eq.

(A12), which should be minimized over to lower bound the key rate.

APPENDIX B: SECURITY AGAINST BASIS-DEPENDENT SOURCE

Here we derive Eq. (28) in Sec. IV. Rewriting Eq. (9) of [34] gives

$$\sqrt{F} \le \sqrt{(1 - \delta_{bx})(1 - \delta_{pz})} + \sqrt{\delta_{bx}\delta_{pz}}, \tag{B1}$$

where F is the fidelity between the two states with two bases (X and Z) sent by Alice, δ_{bx} is the QBER of X-basis states from error testing, and δ_{pz} is the phase error rate of Z-basis states.[2] Similarly, we have another inequality between the QBER of Z-basis states δ_{bz} and the phase error rate of X-basis states δ_{px},

$$\sqrt{F} \le \sqrt{(1 - \delta_{bz})(1 - \delta_{px})} + \sqrt{\delta_{bz}\delta_{px}}. \tag{B2}$$

Adding Eqs. (B1) and (B2) gives

$$\begin{aligned}
\sqrt{F} &\le \frac{1}{2}(\sqrt{(1 - \delta_{bx})(1 - \delta_{pz})} + \sqrt{\delta_{bx}\delta_{pz}} + \sqrt{(1 - \delta_{bz})(1 - \delta_{px})} \\
&+ \sqrt{\delta_{bz}\delta_{px}}) \le \sqrt{(1 - (\delta_{bx} + \delta_{bz})/2)(1 - (\delta_{pz} + \delta_{px})/2)} \\
&+ \sqrt{(\delta_{bx} + \delta_{bz})/2(\delta_{pz} + \delta_{px})/2} = \sqrt{(1 - \delta_b)(1 - \delta_p)} \\
&+ \sqrt{\delta_b \delta_p},
\end{aligned} \tag{B3}$$

where the second inequality is due to the concavity of the function $\sqrt{(1-x)(1-y)} + \sqrt{xy}$ in $[0,1] \times [0,1]$ and we have used the definitions $\delta_b \triangleq (\delta_{bx} + \delta_{bz})/2$ and $\delta_p \triangleq (\delta_{pz} + \delta_{px})/2$. Here we assume that the number of received qubits with Z basis and X basis is the same.

APPENDIX C: RESIDUE FOR THE DECOY+GLLP +RECURRENCE SCHEME

We calculate the residues K_i in Eq. (40) for the five cases $V \otimes S$, $S \otimes V$, $S \otimes S$, $S \otimes M$, and $M \otimes S$. Here, we apply each case, with parameters shown in Table II, in Eq. (A12) to calculate each K_i.

$V \otimes S$. The probability of this case is $\Omega_{VS} = \Omega_V \Omega$:

$$\begin{aligned}
K_{VS} &= 1 - \frac{1}{4} - \frac{1}{4}H_2(1 - 2q_{11}^V) \\
&- \frac{1}{4}H_2(2q_{11}^V) - \frac{1}{4}(1 - e_1)H_2\left(\frac{e_1 - a}{1 - e_1}\right) - \frac{1}{4}e_1 H_2\left(\frac{a}{e_1}\right) \\
&\ge \frac{1}{4} - \frac{1}{4}(1 - e_1)H_2\left(\frac{e_1 - a}{1 - e_1}\right) - \frac{1}{4}e_1 H_2\left(\frac{a}{e_1}\right) \tag{C1}
\end{aligned}$$

with equality when $q_{11}^V = 1/4$. This is due to the concavity of the function $H_2(\cdot)$.

$S \otimes V$. The probability of this case is $\Omega_{VS} = \Omega_V \Omega$:

$$\begin{aligned}
K_{SV} &\ge 1 - \frac{1}{4} - \frac{1}{2}(1 - e_1)H_2\left(\frac{e_1 - a}{1 - e_1}\right) - \frac{1}{2}e_1 H_2\left(\frac{a}{e_1}\right) \\
&- \frac{1}{4}(1 - e_1)H_2(1 - 2q_{11}^V) - \frac{1}{4}e_1 H_2(2q_{11}^V) \\
&\ge \frac{1}{2} - \frac{1}{2}(1 - e_1)H_2\left(\frac{e_1 - a}{1 - e_1}\right) - \frac{1}{2}e_1 H_2\left(\frac{a}{e_1}\right) \tag{C2}
\end{aligned}$$

with equality when $q_{11}^V = 1/4$.

$S \otimes S$. The probability of this case is $\Omega_{VV} = \Omega^2$:

$$\begin{aligned}
K_{SS} &= 1 - e_1(1 - e_1) - \frac{1}{2}(1 - e_1)H_2\left(\frac{e_1 - a}{1 - e_1}\right) - \frac{1}{2}e_1 H_2\left(\frac{a}{e_1}\right) \\
&- \frac{1}{2}(1 - e_1)^2 H_2\left(\frac{e_1 - a}{1 - e_1}\right) - \frac{1}{2}e_1^2 H_2\left(\frac{a}{e_1}\right). \tag{C3}
\end{aligned}$$

$S \otimes M$. The probability of this case is $\Omega_{SM} = \Omega \Omega_M$:

$$\begin{aligned}
K_{SM} &= 1 - \frac{1}{2}e_1(1 - e_M) - \frac{1}{2}e_M(1 - e_1) - \frac{1}{2}(1 - e_1)H_2\left(\frac{e_1 - a}{1 - e_1}\right) \\
&- \frac{1}{2}e_1 H_2\left(\frac{a}{e_1}\right) - \frac{1}{2}(1 - e_1)(1 - e_M)H_2\left(\frac{1 - 2q_{11}^M}{2 - 2e_M}\right) \\
&- \frac{1}{2}e_1 e_M H_2\left(\frac{q_{11}^M}{e_M}\right) \ge \frac{1}{2} - \frac{1}{2}(1 - e_1)H_2\left(\frac{e_1 - a}{1 - e_1}\right) \\
&- \frac{1}{2}e_1 H_2\left(\frac{a}{e_1}\right), \tag{C4}
\end{aligned}$$

with equality when $q_{11}^M = e_M/2$.

$M \otimes S$. The probability of this case is $\Omega_{MS} = \Omega_M \Omega$:

$$\begin{aligned}
K_{MS} &= 1 - \frac{1}{2}e_M(1 - e_1) - \frac{1}{2}e_1(1 - e_M) \\
&- \frac{1}{2}(1 - e_M)H_2\left(\frac{1 - 2q_{11}^M}{2 - 2e_M}\right) - \frac{1}{2}e_M H_2\left(\frac{q_{11}^M}{e_M}\right) \\
&- \frac{1}{2}(1 - e_1)(1 - e_M)H_2\left(\frac{e_1 - a}{1 - e_1}\right) - \frac{1}{2}e_1 e_M H_2\left(\frac{a}{e_1}\right) \\
&\ge \frac{1}{2} - \frac{1}{2}e_M(1 - e_1) - \frac{1}{2}e_1(1 - e_M) \\
&- \frac{1}{2}(1 - e_1)(1 - e_M)H_2\left(\frac{e_1 - a}{1 - e_1}\right) - \frac{1}{2}e_1 e_M H_2\left(\frac{a}{e_1}\right), \tag{C5}
\end{aligned}$$

with equality when $q_{11}^M = e_M/2$.

Therefore, after combining the GLLP [23], decoy [26], and recurrence [10] methods, the data postprocessing residue rate will be given by, substituting Eqs. (C1)–(C5) into Eq. (40),

---

[2]Note that we have used different notations from those in Ref. [34]. By letting $\delta_1 = \delta_{bx}$ and $\delta_{ph} = \delta_{pz}$, and substituting Eq. (3) of [34], we can recover Eq. (9) of [34] from Eq. (B1).

$$r = -\frac{1}{2}f(p_S)H_2(p_S) - \frac{1}{2}p_S f\left(\frac{\delta^2}{p_S}\right)H_2\left(\frac{\delta^2}{p_S}\right) + K_{VS} + K_{SV} + K_{SS} + K_{SM} + K_{MS} \geqslant -\frac{1}{2}f(p_S)H_2(p_S) - \frac{1}{2}p_S f\left(\frac{\delta^2}{p_S}\right)H_2\left(\frac{\delta^2}{p_S}\right)$$

$$+ \Omega_V\Omega\left[\frac{1}{4} - \frac{1}{4}(1-e_1)H_2\left(\frac{e_1-a}{1-e_1}\right) - \frac{1}{4}e_1 H_2\left(\frac{a}{e_1}\right)\right] + \Omega_V\Omega\left[\frac{1}{2} - \frac{1}{2}(1-e_1)H_2\left(\frac{e_1-a}{1-e_1}\right) - \frac{1}{2}e_1 H_2\left(\frac{a}{e_1}\right)\right] + \Omega^2\left[1 - e_1(1-e_1)\right.$$

$$-\frac{1}{2}(1-e_1)H_2\left(\frac{e_1-a}{1-e_1}\right) - \frac{1}{2}e_1 H_2\left(\frac{a}{e_1}\right) - \frac{1}{2}(1-e_1)^2 H_2\left(\frac{e_1-a}{1-e_1}\right) - \frac{1}{2}e_1^2 H_2\left(\frac{a}{e_1}\right)\right] + \Omega\Omega_M\left[\frac{1}{2} - \frac{1}{2}(1-e_1)H_2\left(\frac{e_1-a}{1-e_1}\right)\right.$$

$$\left. -\frac{1}{2}e_1 H_2\left(\frac{a}{e_1}\right)\right] + \Omega\Omega_M\left[\frac{1}{2} - \frac{1}{2}e_M(1-e_1) - \frac{1}{2}e_1(1-e_M) - \frac{1}{2}(1-e_1)(1-e_M)H_2\left(\frac{e_1-a}{1-e_1}\right) - \frac{1}{2}e_1 e_M H_2\left(\frac{a}{e_1}\right)\right] \qquad \text{(C6)}$$

with equality when $q_{11}^V = 1/4$ and $q_{11}^M = e_M/2$. In order to simplify this formula, we define some variables:

$$B = \frac{1}{2}f(p_S)H_2(p_S) + \frac{1}{2}p_S f\left(\frac{\delta^2}{p_S}\right)H_2\left(\frac{\delta^2}{p_S}\right),$$

$$C = \frac{3}{4}\Omega_V\Omega + \Omega^2(1 - e_1 + e_1^2) + \frac{1}{2}\Omega\Omega_M(2 - e_1 - e_M + 2e_1 e_M),$$

$$D_1 = \frac{3}{4}\Omega_V\Omega + \frac{1}{2}\Omega^2(2 - e_1) + \frac{1}{2}\Omega\Omega_M(2 - e_M),$$

$$D_2 = \frac{3}{4}\Omega_V\Omega + \frac{1}{2}\Omega^2(1 + e_1) + \frac{1}{2}\Omega\Omega_M(e_M + 1). \qquad \text{(C7)}$$

Thus Eq. (41) can be expressed as

$$r = -B + K_{VS} + K_{SV} + K_{SS} + K_{SM} + K_{MS} \geqslant -B + C - F_a \qquad \text{(C8)}$$

where

$$F_a = D_1(1 - e_1)H_2\left(\frac{e_1-a}{1-e_1}\right) + D_2 e_1 H_2\left(\frac{a}{e_1}\right) \qquad \text{(C9)}$$

with equality when $q_{11}^V = 1/4$ and $q_{11}^M = e_M/2$.

To lower bound r in Eq. (C8), we need to find the maximum value of F_a over the free variable a. We are interested in the range of $a \in [0, e_1]$ with $e_1 \leqslant 1/2$. Note that F_a is a concave function of a in the valid range, since a sum of two concave functions is also a concave function, and reflecting and shifting a concave function is also a concave function. Thus, we can take the derivative of F_a with respect to a and set it to zero to find the maximum of F_a. Differentiating F_a with respect to a gives

$$\frac{dF_a}{da} = D_1\left[\log_2\left(\frac{e_1-a}{1-e_1}\right) - \log_2\left(1 - \frac{e_1-a}{1-e_1}\right)\right]$$

$$+ D_2\left[\log_2\left(1 - \frac{a}{e_1}\right) - \log_2\left(\frac{a}{e_1}\right)\right].$$

Setting $2^{dF_a/da} = 1$ gives

$$\left(\frac{1-e_1}{e_1-a} - 1\right)^{-D_1}\left(\frac{e_1}{a} - 1\right)^{D_2} = 1.$$

Denoting the left-hand side as $f(a)$, $f(a)$ is a decreasing function of a since dF_a/da is a decreasing function of a. Therefore, we can use the bisection method to find a such that $f(a) = 1$. The initial range for the bisection method is $[0, e_1]$.

[1] C. H. Bennett and G. Brassard, in *Proceedings of IEEE International Conference on Computers, Systems, and Signal Processing, Bangalore, India* (IEEE, New York, 1984), pp. 175–179.

[2] D. Mayers, J. ACM **48**, 351 (2001); a preliminary version is in *Advances in Cryptology—Proceedings of Crypto '96*, edited by N. Koblitz, Lecture Notes in Computer Science Vol. 1109 (Springer-Verlag, New York, 1996), pp. 343–357; E. Biham, M. Boyer, P. O. Boykin, T. Mor, and V. Roychowdhury, in *Proceedings of the Thirty-Second Annual ACM Symposium on Theory of Computing (STOC'00)* (ACM Press, New York, 2000), pp. 715–724.

[3] H.-K. Lo and H. F. Chau, Science **283**, 2050 (1999).

[4] P. W. Shor and J. Preskill, Phys. Rev. Lett. **85**, 441 (2000).

[5] A. K. Ekert and B. Huttner, J. Mod. Opt. **41**, 2455 (1994); D. Deutsch et al., Phys. Rev. Lett. **77**, 2818 (1996); **80**, 2022(E) (1998).

[6] C. H. Bennett, G. Brassard, S. Popescu, B. Schumacher, J. A. Smolin, and W. K. Wootters, Phys. Rev. Lett. **76**, 722 (1996); **78**, 2031(E) (1997).

[7] D. Deutsch, A. Ekert, R. Jozsa, C. Macchiavello, S. Popescu, and A. Sanpera, Phys. Rev. Lett. **77**, 2818 (1996); **80**, 2022(E) (1998).

[8] D. Gottesman and H.-K. Lo, IEEE Trans. Inf. Theory **49**, 457 (2003).

[9] H. F. Chau, Phys. Rev. A **66**, 060302(R) (2002).

[10] K. Gerd, H. Vollbrecht, and F. Verstraete, Phys. Rev. A **71**, 062325 (2005).

[11] M. Ben-Or, http://www.msri.org/publications/ln/msri/2002/qip/ben-or/1/index.html

[12] R. Renner and R. Koenig, in *Theory of Cryptography: Second Theory of Cryptography Conference, TCC 2005*, edited by J. Kilian, (Springer-Verlag, Berlin, 2005), Lecture Notes in Computer Science Vol. 3378 p. 407.

[13] M. Christandl, R. Renner, and A. Ekert, e-print quant-ph/0402131.

[14] R. Renner, N. Gisin, and B. Kraus, Phys. Rev. A **72**, 012332 (2005).

[15] K. Horodecki, D. Leung, H.-K. Lo, and J. Oppenheim, Phys. Rev. Lett. **96**, 070501 (2006).

[16] M. Ben-Or, Michal Horodecki, D. W. Leung, D. Mayers, and J. Oppenheim, in *Theory of Cryptography: Second Theory of Cryptography Conference, TCC 2005*, (Ref. [12]) pp. 386–406.

[17] MagiQ Technologies, http://www.magiqtech.com/; id Quantique, http://www.idquantique.com/

[18] C. H. Bennett, F. Bessette, G. Brassard, L. Salvail, and J. Smolin, J. Cryptology **5**, 3 (1992).

[19] C. Gobby, Z. L. Yuan, and A. J. Shields, Appl. Phys. Lett. **84**, 3762 (2004).

[20] T. Kimura *et al.*, Jpn. J. Appl. Phys., Part 2 **43**, 11217 (2004).

[21] N. Lütkenhaus, Phys. Rev. A **61**, 052304 (2000).

[22] H. Inamori, N. Lütkenhaus, and D. Mayers, e-print quant-ph/0107017.

[23] D. Gottesman, H.-K. Lo, N. Lütkenhaus, and J. Preskill, Quantum Inf. Comput. **4**, 325 (2004).

[24] M. Koashi, Phys. Rev. Lett. **93**, 120501 (2004).

[25] W.-Y. Hwang, Phys. Rev. Lett. **91**, 057901 (2003).

[26] H.-K. Lo, X. Ma, and K. Chen, Phys. Rev. Lett. **94**, 230504 (2005).

[27] X. Ma, B. Qi, Y. Zhao, and H.-K. Lo, Phys. Rev. A **72**, 012326 (2005).

[28] X.-B. Wang, Phys. Rev. Lett. **94**, 230503 (2005); Phys. Rev. A **72**, 012322 (2005).

[29] J. W. Harrington, J. M. Ettinger, R. J. Hughes, and J. E. Nordholt, eprint quant-ph/0503002.

[30] Y. Zhao, B. Qi, X. Ma, H.-K. Lo, and L. Qian, Phys. Rev. Lett. **96**, 070502 (2006).

[31] A. Khalique, G. M. Nikolopoulos, and G. Alber, eprint quant-ph/0604025.

[32] C. H. Bennett, D. P. DiVincenzo, J. A. Smolin, and W. K. Wootters, Phys. Rev. A **54**, 3824 (1996).

[33] A. R. Calderbank and P. W. Shor, Phys. Rev. A **54**, 1098 (1996); A. M. Steane, Proc. R. Soc. London, Ser. A **452**, 2551 (1996).

[34] M. Koashi, eprint quant-ph/0505108.

[35] H.-K. Lo, H. F. Chau, and M. Ardehali, J. Cryptology **18**, 133 (2005).

[36] E. N. Maneva and J. A. Smolin, eprint quant-ph/0003099.

[37] G. Alber, A. Delgado, N. Gisin, and I. Jex, J. Phys. A **34**, 8821 (2001).

[38] J. Dehaene, M. Van den Nest, B. De Moor, and F. Verstraete, Phys. Rev. A **67**, 022310 (2003).

[39] Eve can selectively surpass all the single-photon signals from Alice, and split all the multiphoton signals, keeping one copy herself and sending the other copy to Bob. In this way, Eve could have an identical copy of what Bob processes, thus breaking the security of the BB84 protocol.

[40] B. Huttner, N. Imoto, N. Gisin, and T. Mor, Phys. Rev. A **51**, 1863 (1995).

[41] G. Brassard, N. Lütkenhaus, T. Mor, and B. C. Sanders, Phys. Rev. Lett. **85**, 1330 (2000).

[42] N. Lütkenhaus and M. Jahma, New J. Phys. **4**, 44.1 (2002).

[43] K. Tamaki and H.-K. Lo, Phys. Rev. A **73**, 010302(R) (2006).

[44] A. K. Ekert, Phys. Rev. Lett. **67**, 661 (1991).

[45] C. H. Bennett, Phys. Rev. Lett. **68**, 3121 (1992).

[46] D. Bruss, Phys. Rev. Lett. **81**, 3018 (1998).

[47] V. Scarani, A. Acin, G. Ribordy, and N. Gisin, Phys. Rev. Lett. **92**, 057901 (2004).

[48] C.-H. F. Fung, K. Tamaki, and H.-K. Lo, Phys. Rev. A **73**, 012337 (2006).

[49] G. Brassard and L. Salvail, Advances in Cryptology, Proceedings of EUROCRYPT '93, 1993 (unpublished).

[50] U. M. Maurer and S. Wolf, IEEE Trans. Inf. Theory **45**, 499 (1999).

[51] H.-K. Lo, Quantum Inf. Comput. **5**, 413 (2005).